Making Direction a First-Class Citizen of Tobler's First Law of Geography

Rui Zhu, Krzysztof Janowicz, Gengchen Mai

STKO Lab

Department of Geography

University of California, Santa Barbara

Abstract

Waldo Tobler frequently reminded us that the law named after him was nothing more than calling for exceptions. This paper discusses one of these exceptions. Spatial relation between points are frequently modeled as vectors in which both distance and direction are of equal prominence. However, in Toblers First Law of Geography (TFL), such a relation is described only from the perspective of distance by relating the decreasing similarity of observations in some attribute space to their increasing distance in geographic space. Although anisotropic versions of many geographic analysis techniques, such as directional semivariograms, anisotropy clustering, and anisotropic point pattern analysis, have been developed over the years, direction remains on the level of an afterthought. We argue that compared to distance, directional information is still under-explored and anisotropic techniques are substantially less frequently applied in everyday GIS analysis. Commonly, when classical spatial autocorrelation indicators, such as Morans I, are used to understand a spatial pattern, the weight matrix is only built from distance without direction being considered. Similarly, GIS operations, such as buffering, do not take direction into account either, with distance on all directions being equally treated. While in reality, particularly in urban structures and when processes are driven by the underlying physical geography, direction plays an essential role. In this paper we ask the question of whether the development of early GIS, data (sample) sparsity, and Tobler's law lead to a theory-induced blindness for the role of direction. If so, is it possible to envision direction becoming a first-class citizen of equal importance to distance instead of being an afterthought only considered when the deviation from a perfect circle becomes too obvious to be ignored.

Keywords: Direction, Anisotropic Modeling, Tobler's First Law of Geography, Isotropicity, Spatial Dependence

1   Introduction

Thanks to the wide use and complex nature of spatial phenomena, detecting, quantifying and modeling spatial patterns have been the fundamental interests for not only geographers, but also researchers from other disciplines such as environmental science, ecology, geology, criminologist, astronomy, material science, and economics. As a guiding principle, Tobler's First Law of Geography (TFL) (Tobler, 1970) is widely accepted as the conceptual foundation of many classic spatial

1

models such as distance decay function and inverse distance weighting. Generally speaking, spatial patterns are invariant under transformation, such as *scale*, *translation*, and *rotation*. In spatial analysis, both scale and translation invariance have received significant attentions. For instance, most spatial patterns are known to be scale dependent. Therefore, multiple techniques have been introduced to study scale effects (Atkinson and Tate, 2000; Kyriakidis, 2004; Lee et al., 2018; Wolf et al., 2018; Boeing, 2018a). Similarly, a number of spatial statistics, such as the semivariogram and Ripley's K, are based on assumptions of first- or second-order stationarity i.e., translation invariance (Myers, 1989; Goovaerts, 1997; O'Sullivan and Unwin, 2014). Rotation transformation, in contrast, has been less frequently investigated both theoretically and practically in spatial analysis.

Nonetheless, rotation (in)variance, known as *isotropicity* or *anisotropicity*, plays an equal role in understanding spatial processes and patterns as compared to scale and translation transformations. Criminologists, for instance, have long noted the importance of anisotropicity in considering distance decay, e.g., when predicting the home (or work) location of culprits based on the location at which they committed the crime (Rengert et al., 1999). People do not operate in an abstract isotropic plane but a highly anisotropic environment shaped by transportation infrastructure, terrain, accessibility, and so on. Put differently, if one would rotate the activity space where a culprit conducted crimes, the resulting pattern would look differently. The same can be said about events such as wildfires. Consider the major Thomas Fire affecting Southern California in December 2017 as an example; see Figure 1. While relatively few people were affected by the fire as such, hundreds of thousands were affected by the air pollution caused by the smoke. The air pollution warnings, however, were by no means evenly distributed over Southern California but varied greatly by day due to wind direction as well as factors such as terrain and elevation, which are not isotropic either. Communities to the west of the fire were heavily affected (during the time the picture was taken) even if they were more than 80 miles away, while communities in direct proximity to the fire but situated to the east remained largely unaffected. One could argue that anisotropic patterns are the rule, not the exception.

In this paper we present a series of thought experiments asking the question of whether the development of early GIS, data (sample) sparsity, and Tobler's law lead to a *theory-induced blindness* (Kahneman and Egan, 2011) for the role of direction. If so, is it possible to envision direction becoming a first-class citizen of equal importance to distance instead of being an afterthought only considered when the deviation from a perfect circle becomes too obvious to be ignored? Do notions such as *neighborhood* and *decay* exist in a purely directional framework? Do origin-destination flows cluster differently when considering global instead of local reference frames for direction? Furthermore, we will present a version of TFL based on collinearity that takes distance and direction into account and can be regarded as a generalization of the initial law.

The paper is structured as follows. Section 2 reexamines how isotropicity is approached in common spatial analysis. In Section 3, we review research and techniques that explicitly consider direction. A series of thought experiments about direction-based techniques are proposed and experimented in Section 4. Finally, in Section 5 we conclude the paper and discuss directions for future research.

Figure 1: Smoke from the Thomas Fire, Dec 2018 (earthobservatory.nasa.gov)

2 Rethinking Assumptions of Isotropicity

In this section, we will revisit the basic assumption of isotropicity as applied to geographic space.

2.1 Types of Isotropicity

In spatial analysis, we often operate under assumptions such as distances being symmetric, point patterns being derived from Poisson processes, and geographic fields being realizations of 2D Gaussian processes. Interestingly, these assumptions often also imply isotropicity as an additional assumption. Isotropicity can be defined as invariance to rotation: $f(\mathbf{x}') = f(\mathbf{R}\mathbf{x}) = f(\mathbf{x})$, where $\mathbf{R}$ is the rotation matrix. It is often convenient to distinguish between two types of isotropicity: *stationary isotropicity*, where isotropicity is observed locally, and *radial isotropicity* with a global origin (Baddeley et al., 2015). Hence, stationary isotropicity implies translation invariance, while radial isotropicity does not. As shown in Figure 2, the homogeneous Poisson process (left) exhibits stationary isotropicity, while the point pattern (right) shows radial isotropicity, with tree rings being a common example. One can think of the first case as rotations around local origins.

2.2 Spatial Isotropicity as An Oversimplification

Waldo Tobler challenged the validity of assuming isotropicity in geographic modeling in 1990s (Tobler, 1993). He argued that with an increasing number of available geosopatial data and the

rapid emergence of GIS, simplified assumptions about geographic space being isotropic should be reconsidered. For instance, the concept of *cost* (e.g., travel time), which acknowledges geospatial factors such as slope, terrain, and transportation mode, was proposed in addition to merely using Euclidean distance. Tobler's argument, however, was more focused on the isotropic plane assumption, without explicitly discussing processes acting on geographic space. Hence, assuming an underlying process in the physical world to be isotropic, will potentially yield oversimplified isotropic patterns.

In fact, numerous physical geospatial processes and patterns, such as air pollution proliferation (Lin et al., 2018), city dynamics (Cranshaw et al., 2012; Yan et al., 2017), and human mobility (Song and Miller, 2014) are inherently anisotropic. For example, winds affect the proliferation of air pollution in different directions and human movement is restricted by transportation infrastructure. However, researchers normally study these processes with an isotropic assumption. Lin et al. (2018) for instance proposed a geo-context based diffusion convolution recurrent neural network to forecast short-term $PM_{2.5}$ concentrations, in which circle bufferings are established as spatial contexts such as houses and green land. A similar isotropic buffering method has been used by Yan et al. (2017) to capture the spatial context of Points Of Interest (POIs) in order to learn embeddings for place types. In research about city dynamics, such as the Livehoods project (Cranshaw et al., 2012), neighborhoods were commonly constructed using isotropic approaches (e.g., spectrual clustering). However, we barely observe isotropic neighborhoods in reality due to the complex interaction between humans and their environment. Likewise, Song and Miller (2014) investigated the visiting probability distribution of individuals by adopting the space-time prism, in which individuals again were assumed to move in an isotropic geographic space.
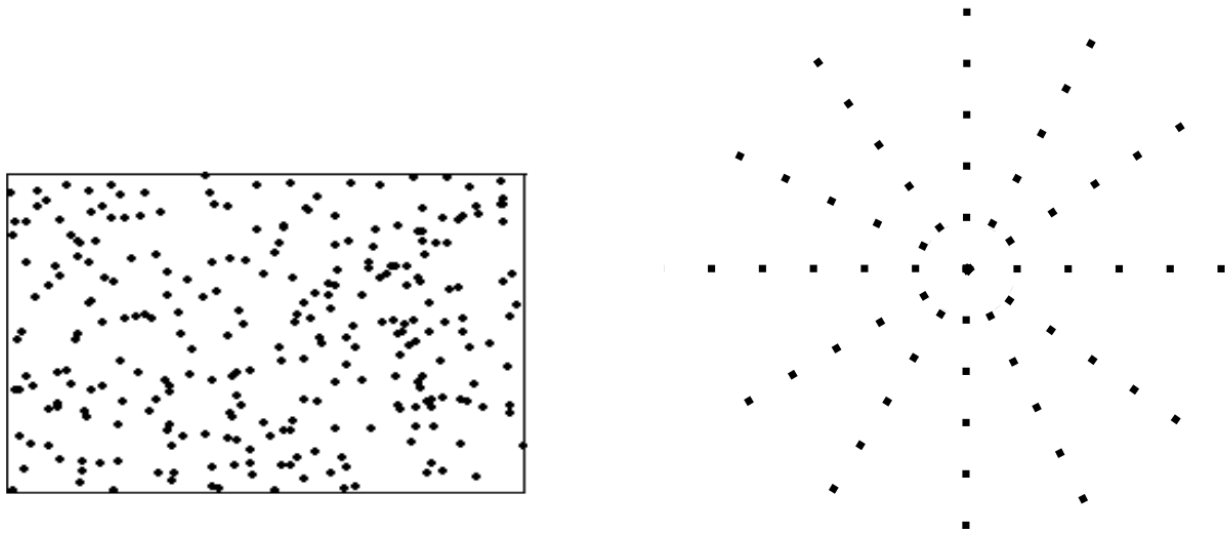

Figure 2: Left: stationary isotropicity. Right: radial isotropicity

The same argument can be made about GIS operations and algorithms which are also operated under the assumption of isotropicity. For example, Figure 3 shows a spatial point pattern of crimes conducted in Austin, Texas, USA in 2016. Despite the observation that the resulting point patterns are anisotropic, there is no option in ArcMap to construct anisotropic buffers around these crime

scenes, e.g., to estimate the location of an offender. Other similar cases include average nearest neighbor, inverse distance weighting, clustering, and hot spot analysis, and such a limitation is frequently observed in other popular GIS softwares/services as well such as Quantum GIS and GRASS. Nevertheless, it is worth noting that for some of these operations, anisotropic options are theoretically available but have not yet been implemented. For instance, there is recent interest in anisotropic clustering and point pattern analysis (Mai et al., 2018; Rajala et al., 2018).
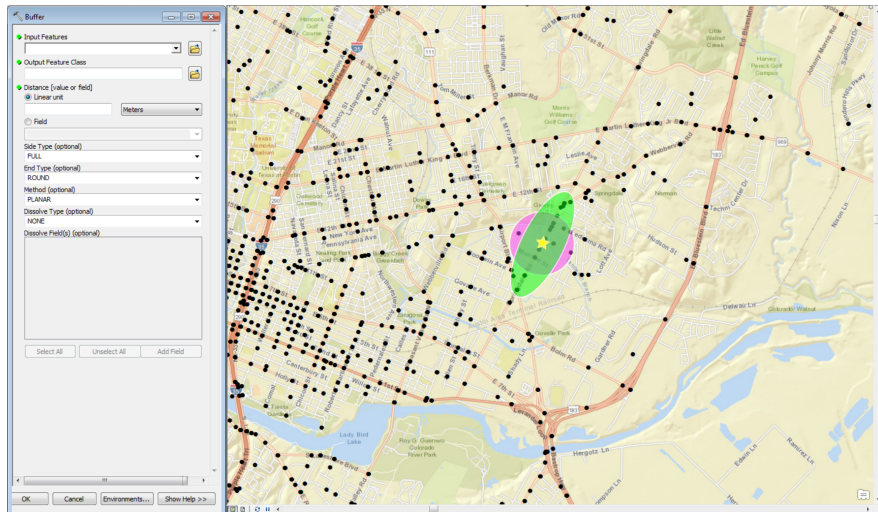

Figure 3: Buffer tool in ArcMap with the crime pattern at Austin (2016). Pink circular buffer is generated from the tool, and the green elliptical buffer is the ideal one.

With respect to studying spatial patterns, the majority of spatial indicators are based on distance only, e.g., Moran's I and LISA (Moran, 1950; Geary, 1954; Getis, 1991; Getis and Ord, 1992; Anselin, 1995; Sawada, 2001). Indicators that relate angular effect to spatial dependence are rare.

In summary, given the complexity of geographic space, spatial processes and patterns, the assumption of isotropicity in spatial analysis, albeit often useful, is an oversimplification. GIS tools are primarily implemented following the isotropic assumption, sometimes offering adjustments for anisotropicity as options.

2.3 Reasons to Assume Isotropicity

Compared to distance, direction is more challenging to model and computationally more demanding. Distance is a relation between two locations, while direction requires at least three (e.g., two targets plus the origin to form an angle) thereby requiring a larger sample size. Specifically, when the sample size is small, it is difficult to have enough replicates for statistical analysis on directional information, thus the assumption of isotropicity is often made for spatial analysis (Rajala et al., 2018). One can regard directional analysis as higher ordered. Put differently, the ability to analyze more complex patterns increases the computational demands (Kaito et al., 2015; Zhu et al., 2017). Moreover direction is measured on a cyclical ratio scale (Chrisman, 1998). Similarly, the notion of a direction based (or even just anisotropic) neighborhood is less intuitive. Finally, directional dependency varies greatly by (geographic) scale. For instance, directional information may play a role only at large scales, such as the patterns of plants (Illian et al., 2008) while

in other cases directional dependency is significant only at small scales such as individual-level crime patterns (Rengert et al., 1999). Many of these arguments and potential reasons have become less relevant given progress in (parallel) algorithm design, big data, inexpensive instrumentation, a data sharing culture, and so forth, and this has likely contributed to the growth of anisotropic techniques over the past 10 years. Last but not least, from a conceptual perspective, the lack of a directional component in TFL may have led to a theory-induced blindness, where we focus on distance first and only consider direction as an afterthought. However, it *is* possible to consider direction within TFL. For instance, if the parameterization of distance decay varies as a function of direction, isotropicity is defined as the case where this variation is negligible.

Therefore the concepts of *(an)isotropicity* and *directional dependence* should be at the same level as *stationarity / homogeneity* and *spatial dependence* in spatial analysis.

3   Where Direction Has Been Considered

Noticing the importance of direction in spatial analysis, a number of researchers have developed anisotropic/direction-based techniques to address various problems. Bennett et al. (1985) categorized spatial analysis into two models: *spatial interaction* and *spatial structure*. Direction is explicitly encoded in the former case, such as flows and trajectories but not in the latter case with spatial point patterns and geographic fields as examples. Even though directional information could facilitate the modeling of both spatial interactions and structures, it is worth noting that most existing techniques still rely on distance-based approaches and assume isotropicity. This section reviews work that employs directional information on either of these two categories. In addition, direction has also been investigated by various subfields of geography, such as spatial reasoning and GIS operations (see Section 3.3). Our goal is to provide an overview of how direction has been approached in the literature.

3.1   Directions in Spatial Interactions

Spatial interaction is defined as *flows* between geographic entities (Haynes et al., 1984; Wilson, 1971; Tobler, 1975; Roy and Thill, 2004). Examples of these flows include students traveling from one state to another, the demand/supply between two markets, birds migration, and so on. Although direction is implicitly encoded in these data, only a few studies have taken direction into account explicitly when modeling flows. The asymmetry of spatial interactions inspired Tobler (1975) to investigate an algebraic approach to quantifying and subsequently visualizing the vector field of flows, in which the role of direction has been emphasized. However, the paper does not discuss how directional information could be modeled to assist the understanding of flow patterns.

Another example of spatial interaction are movement studies. Murray et al. (2012) explored the pattern of movements in space and time using circular statistics, in which the bi-variate movement vectors (i.e., distance and direction) were partitioned into different distance-direction regions of a circle. They proposed a goodness-of-fit testing to statistically check the deviation of observed pattern to the expected one. Applying the approach to residential housing movement data, Murray et al. (2012) discovered both distance decay effects and the anisotropicity. In lieu of evaluating the general distance-direction pattern of movements, Liu et al. (2015) proposed spatial autocorrelation indicators to test the association of flow vectors globally and locally, by extending Moran's

I (Moran, 1950) and LISA (Anselin, 1995), respectively from the scalar version to a vector one. To use Moran's I as an example, both the magnitude and direction of movement flows were considered by replacing the product of scalar deviation between two locations to the mean with a dot product of the vector deviation of two flows to the mean. Nonetheless, the spatial weight matrix for flow was solely defined by a distance-based neighborhood using the origin or destination.

Motivated by clustering spatial flows, multiple approaches were introduced to calculate the similarity between flow vectors (Zhu and Guo, 2014; Tao and Thill, 2016; Gao et al., 2018; Yao et al., 2018). Notwithstanding, barely any of them have direction being explicitly considered, which could cause misinterpretation of the pattern (see detailed discussions in Section 4.1). Tao and Thill (2016) proposed a similarity measure as a combination of flow length and spatial proximity. Even though direction was not explicitly employed in their model, they discussed how direction was implicitly inferred by the distance between origin-origin and destination-destination pairs. Another current work that incorporated direction was presented by Yao et al. (2018), in which directional information were converted to distances between the two destinations with their origins being translated to be the same.

3.2   Directions in Spatial Structures

In contrast to spatial flows, direction is not explicitly defined in many other types of spatial data. In this section, we review techniques that explore the role of anisotropicity in geographic fields and spatial point patterns.

Focusing on geostatistical data, Isaaks and Srivastava (1989) and Goovaerts (1997) categorized anisotropic models into geometric anisotropy, in which only the range of the semivariagram changes with direction but not the shape and sill, and zonal anisotropy, in which both range and sill depend on direction. Numerous techniques were introduced to deal with these two cases, all of which were based on rotational and scaling transformations such that distance was converted from an anisotropic space to an isotropic one. To generalize anisotropic modeling, Eriksson and Siska (2000) investigated the ellipses in an attempt to consistently model the directional varying parameters such as sill, range, nugget, and power in an universal framework. In addition to modeling anisotropicity globally in the sense of fitting the semivariogram, there is an increasing number of work aiming to model locally varying spatial anistropy as well (Te Stroet and Snepvangers, 2005; Boisvert and Deutsch, 2011; Bongajum et al., 2013), by which more complicated spatial patterns could be revealed such as channels and veins from geological deposits.

To analyze spatial point patterns, researchers categorize the mechanisms of anisotropic patterns into geometric anisotropy, where points are converted from a stationary and isotropic pattern by a rotational transformation, and oriented clusters, where the intensity of points increases along a direction (Lawson et al., 2007; Illian et al., 2008; Rajala et al., 2018). Anisotropic approaches, such as Fry plots (Fry, 1979), nearest neighbor orientation density (Illian et al., 2008), angle dependent K function (Ohser and Stoyan, 1981), spectral (Bartlett, 1964) and wavelet (Rosenberg, 2004) analysis were developed to achieve a broad range of analysis, including the detection of anisotropicity, testing for isotropicity, and estimation of the direction of point patterns. However, it is worth noting that despite direction being considered, distance dominates in most of these techniques with direction being regarded as one type of point marks similar to other associated attributes.

3.3 Further Uses of Direction

Beyond quantifying directional information to improve the understanding of spatial patterns, direction also plays a role in fields such as spatial reasoning, GIS operations, geospatial semantics and spatial networks. For example, Frank (1992) proposed a qualitative approach to conduct spatial reasoning based on both cardinal direction and qualitative distance. In contrast to quantitatively measuring the role of direction in classic spatial analysis, this work explored qualitative reasoning of space using directions. Furthermore, there are endeavors to extend normal spatial buffering to its anisotropic version. One example is Mu (2008), which introduced an anisotropic buffering process by allowing the distance to be relative along different directions, with the goal of making sure the buffering process along all directions simultaneously reaches the boundary of Voronoi polygons built from a geometry set. For instance, if a geometry's Voronoi polygon had a shape that is elongated along west-east direction, then the generated buffer for this geometry would have greater length along west-east direction. Spatial clustering is another type of classic GIS operations. By replacing the circular searching window by an ellipse, Mai et al. (2018) proposed an anisotropic version of the DBSCAN algorithm, which is able to detect clusters of points that have an arbitrary geometry, such as points of interest along a street. With respect to geospatial semantics, Zhu et al. (2016) proposed spatial signatures that incorporated direction-based statistical analysis, such as standard deviational ellipse, to understand the semantics of geographic feature types. Studies of spatial networks have to leverage the embedded direction of edges in order to characterize patterns (Gastner and Newman, 2006; Barthélemy, 2011; Barthelemy, 2018). To incorporate the topology and structure of spatial networks, Ermagun and Levinson (2018a,b) introduced a network weight matrix in which the edge direction is explicitly considered. A classic application of spatial networks are the road networks; Boeing (2018b) explored the distribution of road directions ~~of road networks~~ in urban cities and discovered that directional patterns of roads varied among different cities, which can be applied as one factor to characterize urban configurations. In cellular automaton based spatial simulation, directional information has also been rarely incorporated. A notable exception is Clarke's wok on the growth of urban areas by introducing slope resistance and road gravity factors (Clarke et al., 1997).

4 Thought Experiments

As discussed in Section 2, direction could be studied in two scenarios: *stationary isotropicity* (or *local direction*), where rotational origins are constructed for each local study location or region, and *radial isotropicity* (or *global direction*), where only one global origin is defined and all study locations or regions share it, e.g., Grid North. Accordingly, there are two alternatives to include direction in spatial analysis. First of all, directional information can be studied globally, in which the primary tasks are to detect, test, and estimate the directional trend of a pattern in a global sense. Secondly, direction of, for example, vectors, points, or cells can be defined locally, and then their aggregated patterns and/or associations are investigated. In Section 3, we discussed techniques that were developed in various fields that consider direction when characterizing spatial patterns either globally or locally. In this section, we will demonstrate the impact of different approaches to incorporating direction by a series of thought experiments. Our goal here is to provide new perspectives on modeling spatial information emphasizing the role direction could play as a first-

class citizen in spatial analysis *without* implying that direction-only techniques should replace those based on distance.

4.1 Spatial Interactions

In Section 3.1, we introduced two recent approaches for measuring the similarity of flow vectors, with directional information either explicitly or implicitly embedded. As a thought experiment, we discuss their potential drawbacks and showcase alternative formulations that will allow users to distinguish previously indistinguishable origin-destination flows.

First, Tao and Thill (2016) promoted a flow similarity measure (Formula 1), in which both spatial proximity (i.e., d_O and d_D) and flow lengths (i.e., L_i and L_j) were accounted for. Even though direction was not a factor being directly considered, the authors argue that it was implicitly incorporated in spatial proximity, which is computed as weighted sum of origin-origin (d_O) and destination-destination (d_D) distances. The underlying rational is that when spatial proximity was fixed, the relative direction of the two flows would then be constrained to such a small degree of freedom that including direction would be unnecessary. In the following, we will show that such an implicit model does not capture all cases of directional dependence. Namely, there are flow patterns which are relevant but are challenging to distinguish. For example, the three cases illustrated in Figure 4 yield the same results under Formula 1. Specifically, comparing flow pairs (A_1, B_1) with (A_2, B_2), the only difference is the direction of the two flows, with A_1 and B_1 being parallel and A_2 and B_2 crossing each other. Hence, since $dis_{A_1 B_1} = dis_{A_2 B_2}$, both flow pairs are equal. Note, however, that two people traveling along routes represented by these flows may have met in the second but not the first case. Likewise, the flow pair (A_3, B_3) has different origin-origin (d_O) and destination-destination (d_D) distances compared to (A_1, B_1). Since Formula 1 considers spatial proximity as weighted sum of the two distances, with the weights suggested to be equal in general (i.e., $\alpha = \beta$), the two pairs would be equal again. However, one can observe an important distinction between pairs (A_1, B_1) and (A_3, B_3): the local directional angle of the two flows (A_3, B_3) causing them to diverge.

$$dis_{ij} = \sqrt{\frac{\alpha d_O^2 + \beta d_D^2}{L_i L_j}} \tag{1}$$

Figure 4: Examples of flow vectors. A and B have the same length (i.e., $L_i = L_j$).

In contrast, Yao et al. (2018) explicitly incorporated direction to characterize flows. However, they only consider a local perspective. Put differently, these approaches assume stationary isotrop-
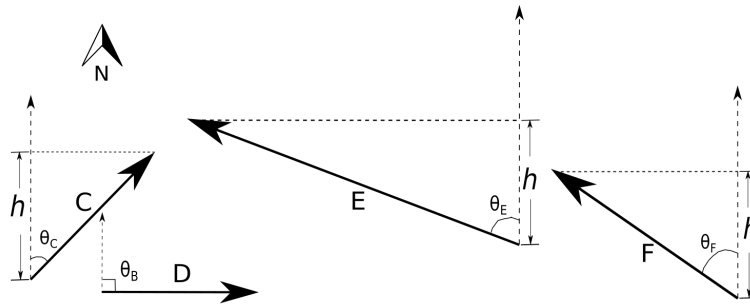
icity, where directions are measured from origins that are defined locally for individual locations or regions such as transportation zones. In radial isotropicity a global origin is defined and all directions are constructed relative to it. Next we will approach flow patterns from such a global perspective. As Figure 5 (top) shows, despite the fact that flows C, E and F are distinct in terms of vector length, spatial proximity and their local directional angle, they all orient close to the True North. In contrast, flow D is more similar to C in respect to all the three aforementioned factors; however its different global orientation makes it dissimilar from the rest. However, if only local direction would be employed (Figure 5, bottom), in which all the four flows were translated to the same locally defined origin O first, D would end up to be more similar to C compared to E and F due to the relation of $\theta_{CD} < \theta_{CE} < \theta_{CF}$. To address this issue, we introduce a new indicator shown as Formula 2 here, in which both global direction $(\cos(\theta))$ and flow length (L) are taken into account to quantify the dissimilarity between two flows i and j. As the top of Figure 5 illustrated, since flow C, E, and F all share the same projected length along the True North (i.e., $h_i = L_i cos(\theta_i) = h \neq 0, i = C, E, F$), their pairwise dissimilarities would be 0; while flow D tends to be unique as $h_D = 0 \neq h$. This pattern is not uncommon in reality. For example, when studying the spatial patterns of immigrant flows in the northern hemisphere, it is noticeable that a majority of flows are from south to north (e.g., Mexico to U.S., Maghreb to northern Europe), with only few exceptions (e.g., Malaysia to Singapore). Hence, researchers interested in the mechanisms driving immigration would consider these SN flows to be similar despite the distance of their origins and destinations being thousands of kilometers apart. Put differently, the global flow direction plays a more prominent role in distinguishing and classifying immigrant flows as compared to other factors, such as spatial proximity.

$$dis_{ij} = |L_i \cos(\theta_i) - L_j \cos(\theta_j)| \tag{2}$$

4.2 Spatial Structures

Stationary isotropicity receives more attentions than radial isotropicity in spatial interaction modeling. Conversely, models developed to analyze spatial structures employ radial isotropicity over stationary isotropicity. For example, *geometric anisotropy modeling*, for either spatial point patterns or geographic fields, is inspired by transforming ellipses to circles (see Section 3.2). An ellipse is established globally with only one set of origin, major, and minor axes being determined. For instance, the popular modeling of directional semivariograms (Goovaerts, 1997) is a process of fitting parameters (e.g., range and sill) of the covariance functions differently along selected directions (e.g., cardinal directions). These are defined relative to one global origin and reference system. However, it is also feasible to model semivariograms in the context of stationary isotropicity. What information could a directional semivariogram convey, when the direction for each location is defined based on its local origin (e.g., the location itself)? As Figure 6 illustrates, the other two points (in spatial point patterns), or cells (in geographic fields), s_j and s_k have to be selected in an attempt to construct the local angle for location s_i. From this perspective, there are clear relations to Multi-Point Geostatistics (MPS) and the ideas of geo-multipoles (Zhu et al., 2017).
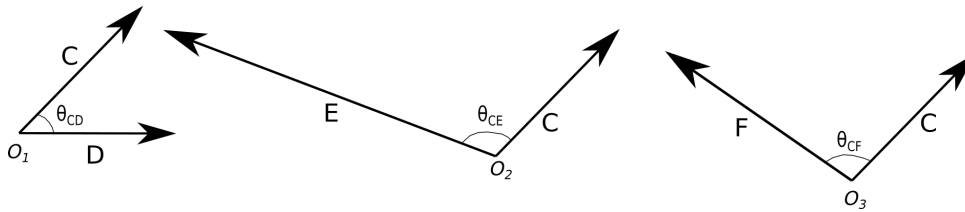
Figure 5: Examples of flow vectors. Top: global direction is considered ($\theta_C = \theta_E = \theta_F < \theta_B$). Bottom: local direction is considered ($\theta_{CD} < \theta_{CF} < \theta_{CE}$).
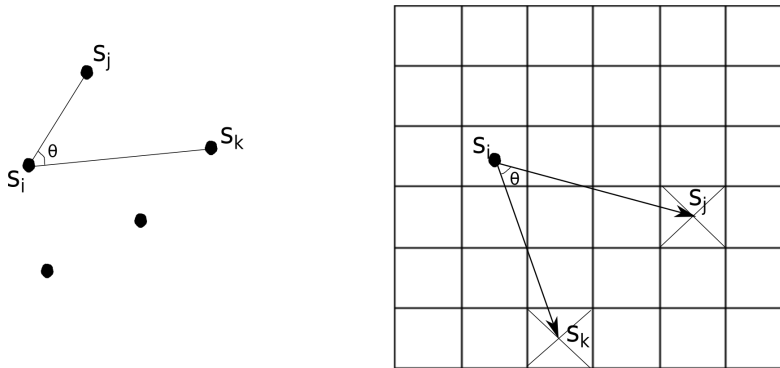

Figure 6: Examples of locally defined directional angles for s_i. Left: a spatial point pattern. Right: a geographic field modeled as raster.

Figure 7 illustrates an experiment of comparing the conventional directional semivariogram with a version in which the direction is defined as local angles of two pairs (i.e., comprised of three locations). The selected experimental data was first introduced by Burrough and McDonnell (1986) and has been widely used to demonstrate geostatistic methods. The top figure shows the spatial distribution of zinc concentration of 155 sample points collected along the flood plain of the Meuse river. The bottom left of the figure demonstrates the four directional experimental semivariograms,

and the right shows the proposed version with local angles grouped into four classes. It should be noted that even though the distance class (i.e., x-axis) for these two diagrams are set up to be the same, their target statistics (i.e., y-axis) are designed to be different. Since three locations are used to compose directional angles, there is strictly speaking no semivariance (i.e., attribute variance of two locations). Instead, we use formula (3) to make our point.

$$\gamma(s_i|s_j, s_k) = 1 - \frac{(z(s_i) - z(s_j))^2}{(z(s_i) - z(s_k))^2} \tag{3}$$

where $z(\cdot)$ is the associated attribute value at a location, and $z(s_i) - z(s_j) < z(s_i) - z(s_k)$

This statistic could be interpreted in analogy to the *eccentricity* (squared version) of an ellipse, where the origin is at s_i, the length of the minor axis (i.e., $z(s_i) - z(s_j)$) is defined as the relatively smaller attribute difference of the two pairs (s_i, s_j) and (s_i, s_k), and the major axis is the larger one (i.e., $z(s_i) - z(s_k)$). Analogue to geometric anisotropy, this statistic (*pair variance*) quantifies how varied two pairs are in terms of their attribute values.

At least three observations can be made considering such local directional perspective, First, similar to the directional semivariogram, its local version, embraces comparatively different trends towards various local angle groups. Secondly, except for the angle group of 90 to 135 degree, the pair variance (i.e., γ) appears to be independent of distance. However, it can be seen that the mean pair variances across different distance classes vary among the three diagrams, with the group of the largest angle range, 135 to 180 degree, having the largest mean variance, 45 to 90 degree the intermediate, and 0 to 45 the smallest. Simply put, the pair variance, or equally the local anisotropicity, increases with increased angles for these three angle groups. This observation in fact correlates with the general distance effect introduced by TFL, due to the relation between angles and distance (i.e., edge length) in a triangle. The most intriguing observation, however, comes from the angle group of 90 to 135 degree, in which the pair variance is dependent on distance. Specifically, the pair variance starts to increase with distance until around 500 meters, from which the trend begins to decline. This observation reveals the complex shape of the study region (i.e., a big curve at the bottom) and the distribution of those marked points (i.e., along the river).

4.3   Distance-free Approaches

So far we have examined different means by which both global and local notions of direction can facilitate our understanding of spatial patterns. One common feature of these approaches is that they remain dependent on distances primarily, with direction being included additionally (as in the case above where increased angles increase the edge length). Since we argue that the role of direction should be raised to the same level as distance, this section attempts to imagine a thought experiment where distance is not considered at all.

4.3.1   Angular Variogram

Although both the directional semivariogram and its local version have considered direction, distance keeps playing a dominant role in the modeling, which could be reflected by the fact that extracted relations from these diagrams are between the target statistics (e.g., semivariance or pair
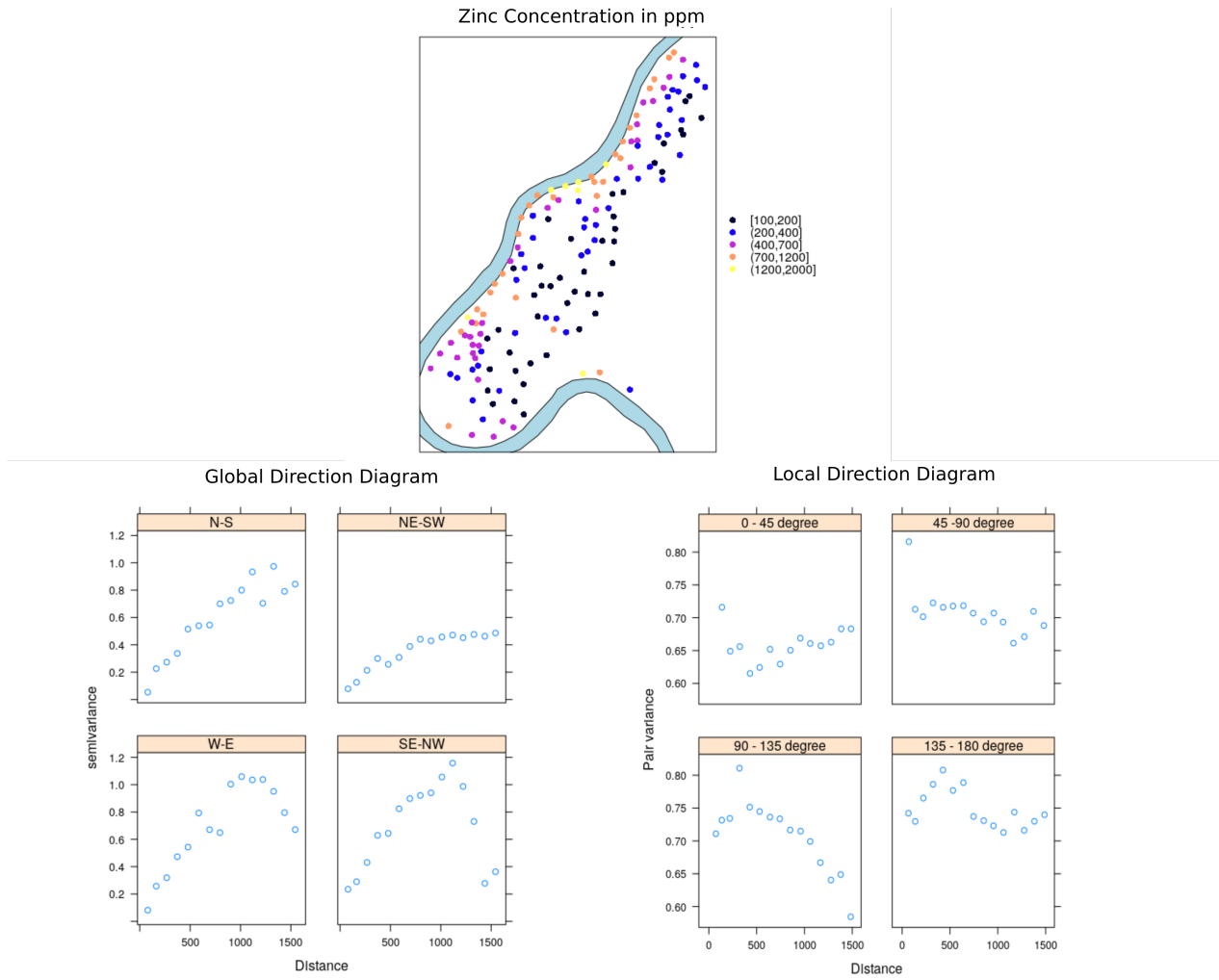
Figure 7: Comparison between the classical *directional semivariogram* and *local* directions.

variance) and distances. The dependence between these statistics and direction has not been directly revealed yet, which, however, could potentially be leveraged to analyze spatial patterns. Consequently, this section envisions a distance-free variogram, where the relation between pair variance (see Formula 3) and local directional angles are plotted. Ideally, for a pattern with n locations, there should be $\binom{n}{3}$ combinations of triangles, and since each triangle has three inner angles, there are in total $\binom{n}{3} \times 3$ combinations of pairs. Due to the exponential nature of this combination (e.g., a 100×100 DEM results in about 499 billion possible combinations), we apply a sample strategy. Specifically, for each location (e.g., cell), we randomly generate one sample pairs for each angle class, and at the end discard those locations that have no pairs for any of the angle class, which is mainly due to the edge effect.

Figure 8 illustrates the envisioned angular variogram using three patterns with different degrees of randomnesses. The pattern on the left is a DEM from the area of Lake Tahoe, CA, which shows a valley along the north-east direction. As the diagram indicates, with increasing angles, the pairs' variance increases until hitting the *sill* at about 0.73 around the *range* of 90 degree. This observation is partially due to the curvilinearity of the valley. To further illustrate this, we gradually

13

weaken the observed pattern by introducing randomness to it. As Figure 8 shows, when 20% randomness is introduced, the generated angular diagram shows a discrepancy from the original one, with no significant sill being observed. Once the randomness reaches 50%, the trend turns to be unstable showing less correlation between angle and pair variance.cThis comparison affirms the feasibility of angular variogram, and consequently the role of direction in describing spatial patterns. Specifically, the relation between angle and pair variance becomes less significant when greater randomness is introduced.

Furthermore, analogue to distance effect, trends revealed from the angular isotrogram with no randomness (i.e., the Original Pattern) could be interpreted as a *direction effect*, which illuminates the general principle of geospatial phenomena: the angle between two pairs has influence over their similarity; and they would be similar if their angle is smaller. However, it is worth noting that the similar trends observed in angular variogram (direction effect) and semivariogram (distance effect) is not a coincidence. In fact, the three angles and three edge lengths (i.e., distances) in a triangle are correlated, with knowing any three of these six elements would already determine the shape of a triangle. Nonetheless, the value of proposed angular variogram should not be neglected, since it has the ability to model high-ordered interactions through a *shape* that is composed of at least three locations. In contrast, conventional distance-based approaches only concentrate on the relation between two locations, i.e., one pair. With this point in mind, we argue that more sophisticated statistics and visualizations should be proposed to extract and interpret the high-order spatial information modeled by incorporating directions, which is beyond the scope of this work. Moreover, we choose to explore local direction in this experiment, leaving the global version as another promising research direction.
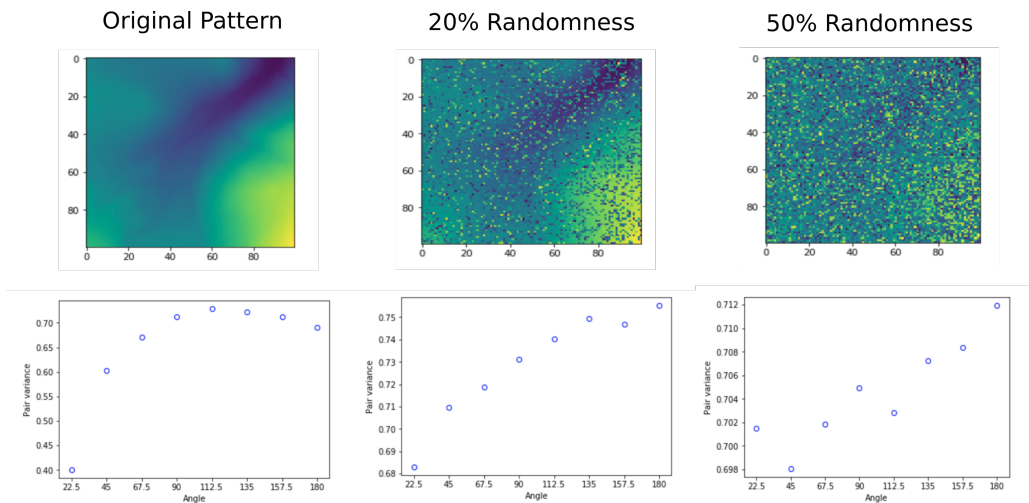

Figure 8: Comparison of angular variogram for patterns with various randomness

4.3.2 Cosine Angular Weighting

According to TFL, closer things are more related. Therefore, one of the simplest spatial prediction models is inverse distance weighting. Even though a circular search neighbor could be replaced by an ellipse, the weighting schema is still based on distance. In this section, we continue our thought experiments by looking at a purely direction-based spatial prediction, which assumes that two pairs

having smaller angle are more related. In lieu of using inverse functions, the trigonometric function $\cos()$ is adopted to model the angular weight. Formula 4 demonstrates using sampled N locations $\{s_j, j = 1...N\}$ to predict the attribute z at unsampled location s_i, where $\{\theta_j, j = 1...N\}$ are the angles between $\overrightarrow{os_i}$ and $\overrightarrow{os_j}$ assuming they have the same global origin o (i.e., radial anisotropicity). Similar to inverse distance weighting, p is a positive power parameter controlling the influence of direction. Due to the symmetric nature of directional influence over 90 degree, e.g., 45 degree has the same influence with 135 degree, the angular weighting function is determined as the absolute of $cos()$.

$$z_i = \frac{\sum_{j=1}^{N} |\cos(\theta_j)|^p z_j}{\sum_{j=1}^{N} |\cos(\theta_j)|^p} \tag{4}$$

To validate the feasibility of *cosine angular weighting (CAW)*, Figure 9 illustrates a synthesized sample data, where the attribute value at red dot s_0 is a target to be predicted, and its neighbors are selected as s_1, s_2, s_3 and s_4. One noticeable characteristic of this data is that s_0, s_1 and s_2 lie on the same direction wrt. the reference system and we assume they share a common value 2; this is analogous to the Thomas fire smoke example. However, since $\overrightarrow{os_3}$ and $\overrightarrow{os_4}$ have directional distortion in regard to the direction of $\overrightarrow{os_0}$, s_3 and s_4 are relatively larger. Therefore, in order to predict the value at s_0, s_1 and s_2 would preferably play a greater role compared to s_3 and s_4. By using CAW, s_1 and s_2 receive larger weights than s_3 and s_4, resulting the value at s_0 as $z(s_0) = \frac{\cos(0) \times 2 + \cos(0) \times 2 + \cos(\pi/8) \times 7 + \cos(\pi/4) \times 10}{\cos(0) + \cos(0) + \cos(\pi/8) + \cos(\pi/4)} = 4.83$. However, if conventional inverse distance weighting (IDW) would have been applied, the result would be: $z(s_0) = \frac{1 \times 2 + (1/3) \times 2 + 1 \times 7 + (1/2) \times 10}{1 + (1/3) + 1 + (1/2)} = 5.17$, keeping in mind that the true value is 2. Note that we set p for both CAW and IDW to be 1, but one would adjust it to control the decaying importance of direction or distance (thereby increasing the difference between the two approaches).

This thought experiment shows how one could utilize direction exclusively in spatial predictions using a rather simple model and a synthesized data set. Whether there would be a need for a purely directional method is out of scope for the work at hand. Meanwhile, new spatial models that incorporate both distance and directional angles could be more promising. Finally, CAW takes a radial isotropicity perspective (i.e., a global perspective), while angles could also be constructed locally with three locations (i.e., two pairs) being studied simultaneously.

4.3.3 Directional Association

As far as spatial association is concerned, distance-based statistics are utilized to quantify the interaction between locations (Getis and Ord, 1992). Even though direction had been used by Costanzo et al. (1983) to illustrate spatial autocorrelation measures of directions (e.g., suspects from similar directions would conduct crimes at places that are close), it is regarded as an *attribute* associated with the location, rather than a factor that model the interaction of locations like distance. In this section, we envision an indicator family (Formula 5) to measure spatial association from a directional perspective, in which classic distance-based spatial interaction is replaced by direction.

$$J = \frac{\sum_{i=1}^{N} \sum_{j=1}^{N} \sum_{k=1}^{N} w(\theta_{ijk}) \gamma(s_i | s_j, s_k)}{\sum_{i=1}^{N} \sum_{j=1}^{N} \sum_{k=1}^{N} w(\theta_{ijk})}, i \neq j \neq k \tag{5}$$
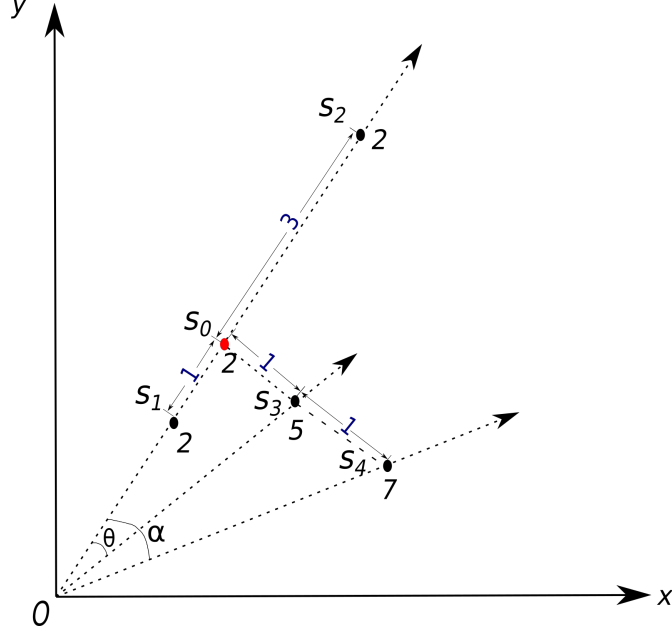
Figure 9: Synthesized points for CAW predication

In Formula 5, s_i, s_j, and s_k are three locations comprising two pairs: $s_i s_j$ and $s_i s_k$; θ_{ijk} repre-sents the angle $\angle s_j s_i s_k$ with s_i as the local origin; N is the number of locations in a spatial pattern; w represents the weight function based on the directional angle; and γ is the attribute interaction model between two pairs. In analogy to Moran' I, J is designed to model how the attribute relation of pairs (i.e., γ) is associated with their directional information (i.e., w). Since three locations are involved in J, one way to compute the attribute interaction γ is to follow Formula 3. For direction-based weight function w, there are multiple possible approaches as well. For example, in Formula 6, and similarity to CAW we use $\cos(\theta_{ijk})$.

$$J = \frac{\sum_{i=1}^{N} \sum_{j=1}^{N} \sum_{k=1}^{N} \cos \theta_{ijk}(1 - \frac{(z(s_i)-z(s_j))^2}{(z(s_i)-z(s'_j))^2})}{\sum_{i=1}^{N} \sum_{j=1}^{N} \sum_{k=1}^{N} \cos(\theta_{ijk})}, i \neq j \neq k \tag{6}$$

The range of J depends on the range of γ. By following Formula 3 (with a range of $[0, 1]$), J would also have the range of $[0, 1]$. Therefore, a J closer to 1 means the pattern tends to have stronger *positive directional association*; namely we expect to find two pairs to be similar if their angle is smaller. On the contrary, it indicates stronger *negative directional association* if J is closer to 0, meaning that one would observe pairs that have larger angles being rather similar. Applying J to the Meuse dataset (see Figure 7) yields 0.64 indicating a (weak) positive directional association.

Similar to distance-based associations, there are multiple alternatives for directional associa-tion by either modifying the angular weight function w or the pair statistics γ. For example, in analogy to contiguity-based neighborhoods, the weight function w could be modeled based on direction-based neighborhoods such that only those locations that are 45 degree to the local origin are regarded as its neighbors. In terms of pair statistics γ, the high-order spatial cumulant (Dimi-trakopoulos et al., 2010) could be incorporated. However, since such an association involves more than two locations, the interpretation would be challenging. Therefore we contemplate that more

robust statistical methods should be studied to assist interpreting and testing directional associations.

4.4 Generalized First Law of Geography

We started by arguing that the strong focus on distance implied by the original formulation of Tobler's First Law, together with other technical limitations such as spatial data sparsity and limitations of early GIS and hardware, may have led to a theory-induced blindness (Kahneman and Egan, 2011) by which we tend to overlook direction initially and only consider it as an afterthought that has to be addressed, e.g., by replacing a scan circle with an ellipse. One could now argue that the very definitions of latitude and longitude, and, thereby, distances on the surface of the earth, include angles already. However, that is not the point we are trying to make. Instead we provided examples to highlight the role of conceptualizing geographic problems and processes by making them *directionally-explicit*. TFL recognizes the role of distance in modeling spatial interactions without examining whether the increasing variance with distance is influenced by direction or not. We believe that a generalized version of Tobler's law can include direction as a first-class citizen without having to make up new laws or radically modifying the existing law [1]. In fact, TFL can be regarded as capturing the case where the role of direction is negligible, e.g., on an abstract plane. In such a case, a generalized version (as a homage, not a replacement) can be derived by making use of *collinearity*.

> *Everything is related to everything else, but near things and those that point into similar directions are more related than distant things and those pointing in different directions.*

Note that we refrain here from distinguishing between local and global notions of direction. Furthermore, staying in line with the vague nature of "near things", we use "those that point into similar directions" to retain the *guiding principle* characteristic of TBL and leave the exact interpretation to specific measures, models, and application needs.

5 Conclusions and Future Work

Variance increases with distance, but it also does so with direction. This, of course, is well known and forms the basis for a wide range of anisotropic techniques in spatial analysis and beyond. Interestingly, however, isotropicity itself is missing from the list of fundamental concepts in GIScience. It received little attention in GIS/GIScience textbooks, Esri's documentation of ArcGIS, and the current GIS body of knowledge. Put differently, anisotropicity remains an afterthought only considered when its consequences on spatial analysis can no longer be ignored. As we illustrated by reviewing the literature, this is not for lack of related research and techniques.

Physical and societal processes do not play out in an abstract isotropic plane. Anisotropicity is the norm, not the exception. In this work, we argued that the fact that direction is not a first-class citizen of foundational concepts such as Tobler's First Law may lead to theory-induced blindness

---

[1] as substantial modifications may destroy the original charm and simplicity of Tobler's First Law.

and believes that direction can be indirectly accounted for by using distance alone. We have high-lighted cases, such as global migration patterns, where this is not the case. We demonstrated that these cases would benefit from making distinctions between local reference frames for directional dependence and global reference frames.

Interestingly many key GIS notions can be modeled with direction alone, such as the direct neighborhood of a cell in Queen's or Rook's case or the ideas of weights and associations more generally. To take this to an extreme, one can even envision purely direction-based interpolation such as in our CAW thought experiment. In fact, we believe that Tobler's first law as such can be generalized in the sense that its original formulation accounts for the case where directional variation is negligible and that deviation from collinearity can be added for cases in which directional variation is significant.

In summary, this work highlights the role of direction and directional dependence as conceptual foundations of GIS processing and analysis. In the future we plan to further investigate similar thought experiments and provide a concrete overview of the role (or lack of it) of anisotropicity in spatial thinking and GIS operations.

6   Bibliography

Anselin, L., 1995. Local indicators of spatial associationlisa. Geographical analysis 27 (2), 93–115.

Atkinson, P. M., Tate, N. J., 2000. Spatial scale problems and geostatistical solutions: a review. The Professional Geographer 52 (4), 607–623.

Baddeley, A., Rubak, E., Turner, R., 2015. Spatial point patterns: methodology and applications with R. Chapman and Hall/CRC.

Barthélemy, M., 2011. Spatial networks. Physics Reports 499 (1-3), 1–101.

Barthelemy, M., 2018. Morphogenesis of spatial networks. Springer.

Bartlett, M., 1964. The spectral analysis of two-dimensional point processes. Biometrika 51 (3/4), 299–311.

Bennett, R. J., Haining, R., Wilson, A., 1985. Spatial structure, spatial interaction, and their integration: a review of alternative models. Environment and Planning A 17 (5), 625–645.

Boeing, G., 2018a. A multi-scale analysis of 27,000 urban street networks: Every us city, town, urbanized area, and zillow neighborhood. Environment and Planning B: Urban Analytics and City Science , 2399808318784595.

Boeing, G., 2018b. Urban spatial order: Street network orientation, configuration, and entropy .

Boisvert, J. B., Deutsch, C. V., 2011. Programs for kriging and sequential gaussian simulation with locally varying anisotropy using non-euclidean distances. Computers & Geosciences 37 (4), 495–510.

Bongajum, E., Boisvert, J., Sacchi, M., 2013. Bayesian linearized seismic inversion with locally varying spatial anisotropy. Journal of Applied Geophysics 88, 31–41.

Burrough, P. A., McDonnell, R. A., 1986. Principles of geographical information systems for land resource assessment .

Chrisman, N. R., 1998. Rethinking levels of measurement for cartography. Cartography and Geographic Information Systems 25 (4), 231–242.

Clarke, K. C., Hoppen, S., Gaydos, L., 1997. A self-modifying cellular automaton model of historical urbanization in the san francisco bay area. Environment and planning B: Planning and design 24 (2), 247–261.

Costanzo, C. M., Hubert, L. J., Golledge, R. G., 1983. A higher moment for spatial statistics. Geographical Analysis 15 (4), 347–351.

Cranshaw, J., Schwartz, R., Hong, J., Sadeh, N., 2012. The livehoods project: Utilizing social media to understand the dynamics of a city. In: Proceedings of AAAI 2012.

Dimitrakopoulos, R., Mustapha, H., Gloaguen, E., 2010. High-order statistics of spatial random fields: exploring spatial cumulants for modeling complex non-gaussian and non-linear phenomena. Mathematical Geosciences 42 (1), 65.

Eriksson, M., Siska, P. P., 2000. Understanding anisotropy computations. Mathematical Geology 32 (6), 683–700.

Ermagun, A., Levinson, D., 2018a. An introduction to the network weight matrix. Geographical Analysis 50 (1), 76–96.

Ermagun, A., Levinson, D. M., 2018b. Development and application of the network weight matrix to predict traffic flow for congested and uncongested conditions. Environment and Planning B: Urban Analytics and City Science , 2399808318763368.

Frank, A. U., 1992. Qualitative spatial reasoning about distances and directions in geographic space. Journal of Visual Languages & Computing 3 (4), 343–371.

Fry, N., 1979. Random point distributions and strain measurement in rocks. Tectonophysics 60 (1-2), 89–105.

Gao, Y., Li, T., Wang, S., Jeong, M.-H., Soltani, K., 2018. A multidimensional spatial scan statistics approach to movement pattern comparison. International Journal of Geographical Information Science 32 (7), 1304–1325.

Gastner, M. T., Newman, M. E., 2006. The spatial structure of networks. The European Physical Journal B-Condensed Matter and Complex Systems 49 (2), 247–252.

Geary, R. C., 1954. The contiguity ratio and statistical mapping. The incorporated statistician 5 (3), 115–146.

Getis, A., 1991. Spatial interaction and spatial autocorrelation: a cross-product approach. Environment and Planning A 23 (9), 1269–1277.

Getis, A., Ord, J. K., 1992. The analysis of spatial association by use of distance statistics. Geographical analysis 24 (3), 189–206.

Goovaerts, P., 1997. Geostatics for natural resources evaluation. Oxford University Press.

Haynes, K. E., Fotheringham, A. S., et al., 1984. Gravity and spatial interaction models. Vol. 2. Sage Beverly Hills, CA.

Illian, J., Penttinen, A., Stoyan, H., Stoyan, D., 2008. Statistical analysis and modelling of spatial point patterns. Vol. 70. John Wiley & Sons.

Isaaks, E. H., Srivastava, R. M., 1989. An introduction to applied geostatistics. Tech. rep., Oxford university press.

Kahneman, D., Egan, P., 2011. Thinking, fast and slow. Vol. 1. Farrar, Straus and Giroux New York.

Kaito, C., Dieckmann, U., Sasaki, A., Takasu, F., 2015. Beyond pairs: Definition and interpretation of third-order structure in spatial point patterns. Journal of theoretical biology 372, 22–38.

Kyriakidis, P. C., 2004. A geostatistical framework for area-to-point spatial interpolation. Geographical Analysis 36 (3), 259–289.

Lawson, A. B., Simeon, S., Kulldorff, M., Biggeri, A., Magnani, C., 2007. Line and point cluster models for spatial health data. Computational Statistics & Data Analysis 51 (12), 6027–6043.

Lee, S.-I., Lee, M., Chun, Y., Griffith, D. A., 2018. Uncertainty in the effects of the modifiable areal unit problem under different levels of spatial autocorrelation: a simulation study. International Journal of Geographical Information Science , 1–20.

Lin, Y., Mago, N., Gao, Y., Li, Y., Chiang, Y.-Y., Shahabi, C., Ambite, J. L., 2018. Exploiting spatiotemporal patterns for accurate air quality forecasting using deep learning. In: Proceedings of the 26th ACM SIGSPATIAL International Conference on Advances in Geographic Information Systems. ACM, pp. 359–368.

Liu, Y., Tong, D., Liu, X., 2015. Measuring spatial autocorrelation of vectors. Geographical Analysis 47 (3), 300–319.

Mai, G., Janowicz, K., Hu, Y., Gao, S., 2018. Adcn: An anisotropic density-based clustering algorithm for discovering spatial point patterns with noise. Transactions in GIS 22 (1), 348–369.

Moran, P. A., 1950. Notes on continuous stochastic phenomena. Biometrika 37 (1/2), 17–23.

Mu, L., 2008. A shape-based buffering method. Environment and Planning B: Planning and Design 35 (3), 399–412.

Murray, A. T., Liu, Y., Rey, S. J., Anselin, L., 2012. Exploring movement object patterns. The Annals of Regional Science 49 (2), 471–484.

Myers, D. E., 1989. To be or not to be... stationary? that is the question. Mathematical Geology 21 (3), 347–362.

Ohser, J., Stoyan, D., 1981. On the second-order and orientation analysis of planar stationary point processes. Biometrical Journal 23 (6), 523–533.

O'Sullivan, D., Unwin, D., 2014. Geographic information analysis. John Wiley & Sons.

Rajala, T., Redenbach, C., Särkkä, A., Sormani, M., 2018. A review on anisotropy analysis of spatial point patterns. Spatial Statistics. Elsevier.0.1016/j.spasta.2018.04.005 .

Rengert, G. F., Piquero, A. R., Jones, P. R., 1999. Distance decay reexamined. Criminology 37 (2), 427–446.

Rosenberg, M. S., 2004. Wavelet analysis for detecting anisotropy in point patterns. Journal of Vegetation Science 15 (2), 277–284.

Roy, J. R., Thill, J.-C., 2004. Spatial interaction modelling. Papers in Regional Science 83 (1), 339–361.

Sawada, M., 2001. Global spatial autocorrelation indices-moran's i, geary's c and the general cross-product statistic. Laboratory of Paleoclimatology and Climatology, Dept. Geography, University of Ottawa,(Mimeo) .

Song, Y., Miller, H. J., 2014. Simulating visit probability distributions within planar space-time prisms. International Journal of Geographical Information Science 28 (1), 104–125.

Tao, R., Thill, J.-C., 2016. Spatial cluster detection in spatial flow data. Geographical Analysis 48 (4), 355–372.

Te Stroet, C. B., Snepvangers, J. J., 2005. Mapping curvilinear structures with local anisotropy kriging. Mathematical geology 37 (6), 635–649.

Tobler, W., 1975. Spatial interaction patterns. Journal of Environmental Systems 6, 271–301.

Tobler, W., 1993. Three presentations on geographical analysis and modeling. National Center for Geographic Information and Analysis. Technical Report , 93–1.

Tobler, W. R., 1970. A computer movie simulating urban growth in the detroit region. Economic Geography 46 (sup1), 234–240.

Wilson, A. G., 1971. A family of spatial interaction models, and associated developments. Environment and Planning A 3 (1), 1–32.

Wolf, L. J., Oshan, T. M., Fotheringham, A. S., 2018. Single and multiscale models of process spatial heterogeneity. Geographical Analysis 50 (3), 223–246.

Yan, B., Janowicz, K., Mai, G., Gao, S., 2017. From itdl to place2vec: Reasoning about place type similarity and relatedness by learning embeddings from augmented spatial contexts. In: Proceedings of the 25th ACM SIGSPATIAL International Conference on Advances in Geographic Information Systems. ACM, p. 35.

Yao, X., Zhu, D., Gao, Y., Wu, L., Zhang, P., Liu, Y., 2018. A stepwise spatio-temporal flow clustering method for discovering mobility trends. IEEE Access 6, 44666–44675.

Zhu, R., Hu, Y., Janowicz, K., McKenzie, G., 2016. Spatial signatures for geographic feature types: Examining gazetteer ontologies using spatial statistics. Transactions in GIS 20 (3), 333–355.

Zhu, R., Kyriakidis, P. C., Janowicz, K., 2017. Beyond pairs: generalizing the geo-dipole for quantifying spatial patterns in geographic fields. In: The Annual International Conference on Geographic Information Science. Springer, pp. 331–348.

Zhu, X., Guo, D., 2014. Mapping large spatial flow data with hierarchical clustering. Transactions in GIS 18 (3), 421–435.